Supporting Information for "Analysis of blue corona discharges at the top of tropical thunderstorm clouds in different phases of convection"

Krystallia Dimitriadou[1], Olivier Chanrion[1], Torsten Neubert[1], Alain Protat[2], Valentin Louf[2], Matthias Heumesser[1], Lasse Husbjerg[1], Christoph Köhn[1], Nikolai Østgaard[3], and Victor Reglero[4]

[1]National Space Institute, Technical University of Denmark (DTU Space), Kgs. Lyngby, Denmark

[2]Australian Bureau of Meteorology, Science and Innovation Group, Radar Science and Nowcasting Team, Melbourne, Australia

[3]University of Bergen, Birkeland Centre for Space Science, Bergen, Norway

[4]University of Valencia, Image Processing Laboratory, Valencia, Spain

Contents of this file

Corresponding author: K. Dimitriadou, DTU Space, Technical University of Denmark, Elektrovej, Building 327, 2800 Kgs. Lyngby, Denmark. (krstd@space.dtu.dk)

Introduction This supplementary information contains plots adding more details to the observations described in the main manuscript. The calculation of the rise times of the blue corona discharges is described thoroughly. For the blue corona discharges accompanied by an elve, we expain in detail what a single and what a double UV pulse mean. Furthermore, we provide information about the atmospheric sounding that characterized the thunderstorm environment which facilitated the formation of blue corona discharges. Last, we describe all the possible errors induced by projection offsets and the different spatial resolutions of the instruments/detectors involved.

1. Rise time calculation

In order to calculate the rise times of the blue corona discharges we implemented an algorithm which processes the whole sequence of ASIM observations in the storm and work as follows:

1. [Find all blue peaks]. It finds all the peaks in the blue photometer that increase by more than 5 $\mu W/m^2$ in 5 samples. The rise time is calculated by counting the number of samples it takes for the blue corona discharge event to increase from 10% of the full amplitude to 90% of the full amplitude

2. [Disregard peaks close to each other] If several peaks occur within 500 samples, it disregards all except the biggest peak.

3. [Disregard delta peaks (cosmic rays)] It sums the blue photometer data together, 100 samples before and after the peak, and take the ratio as (after)/(before). If this ratio is below 2.97, it disregards the blue peak. Note that a lower ratio here suggests highly narrow peaks like cosmic rays.

4. [Disregard peaks where the red photometer is large] It sums blue and red photometer data up 50 samples before the peak and 150 samples after the peak and take their ratio, i.e. sum(phot3[i-50:i+150])/sum(phot1[i-50:i+150]) where i is the peak index. If this ratio is below 0.15 it considers the peak a blue corona discharge.

The threshold value was determined empirically so there is no direct physical reasoning behind the 0.15 threshold. The value was determined by looking at both the photometer data and the camera data. Such ratio allows to filter events by the color, keeping the events that do not contain much red emissions as compared to the blue.

In general, the step 1 results in hundreds of peaks, which then are reduced to tens of peaks in step 2, down to single or no peak in step 3 and 4. All the values in the algorithm are found empirically.

2. Rise time and cloud depth

We first define the cloud depth as the geometrical distance between the light source inside the cloud and the cloud top. The source of the blue emissions that are presented in this paper are thought to originate from cloud depths of less than 1 km below the cloud top. This is calculated as follows: In the Equation (1) of (Soler et al. 2020), if we neglect the absorption for the 337 nm, the maximum is reached at $L^2/(6D)$ and the rise time RT of a blue pulse can be approximated by $0.445L^2/(6D)$, where L and D are the cloud depth and the diffusion coefficient, respectively. This results in $RT = 1.38 \cdot 10^{-11} L^2$ s for a cloud droplet concentration of 10^8 m^{-3} and radii of 15 μm. The cloud depth is therefore a function of the square root of the rise time which can be estimated by $L = 2.7 \cdot 10^5 \sqrt{RT}$.

3. Single and double UV signals

10 out of the 14 blue pulses are associated with a UV signal in the 180-230 nm (VUV) ASIM photometer. Those signals are characterised as either single or double pulses depending on how many peaks are identified. 5 out of 10 of UV signals are double, indicating that the VUV photometer has recorded signals from both the blue discharge and the accompanying elve. The remaining signals are characterized as single pulses. In 3 of them, the VUV photometer records only the signal from the blue discharges emanating from the cloud top. The last 2 single pulses are also attributed to elves.

4. The atmospheric sounding

Figure S1 displays a Skew-T log-P diagram, commonly known as an atmospheric/ balloon sounding or radiosonde. Such diagrams are important both for weather forecasting models and assessing the atmospheric conditions for a given time and place. They provide information regarding the stability or instability of the atmosphere, pinpoint weather elements (temperature, dew point, wind speed and direction etc.) in all layers of the atmosphere as well as important atmospheric indices (CAPE, CIN, K index etc.), important for the categorization of convective environments.

The basic lines that constitute such a diagram are the isobars on the vertical axis, solid lines of equal pressure that run horizontally and with the space between the pressure levels to change, thus log-P. Pressure is mostly given every 100 hPa, but the presented sounding indicates more levels in between. In each pressure level the corresponding altitude is give next to it in metres. Pressure height is preferred instead of the actual typical height, since pressure is not constant in the upper atmosphere (low and high pressure systems). On the horizontal axis, there are the values of the isotherms, solid lines of equal temperature that run vertically. There are three additional types of lines, the saturation mixing ratio lines, the dry adiabatic lapse rates line and the moist adiabatic lapse rate lines which are out of the scope of this study, therefore will not be discussed. Last, on the right of the diagram, the wind barbs are plotted which indicate the wind speed and direction for a given atmospheric layer. A wind bar points to the direction from which the winds are coming. The lines and triangle perpendicular to the wind bars indicate the speed of the

wind. Half line is 5 knots, a full line is 10 knots and the triangle is 50 knots. The wind speed is calculated from the summation of all the lines and triangles.

In the diagram, two intense and one faint black lines are plotted. From left to the right, the first line is the dewpoint plot which shows the quantity of moisture in the air. The second line is the temperature measured in the atmosphere (or environmental sounding) which is always to the right of the dew point line. The faint black curved line is the parcel lapse rate and indicates the path an air parcel will take if raised from the Planetary Boundary Layer (100 m - 2 km). This line is used for the calculation of thermodynamic indices such us CAPE (Convection Available Potential Energy), CIN (Convective INhibition), LI (Lifted Index) etc. CAPE, an index commonly used for characterising convection in storms, is the integration of positive area on a sounding. Positive area is defined as the region where the the parcel temperature (curved thin black line) is warmer than the actual temperature (second line from the left). Depending on how close the dewpoint and the temperature line are, we extract information about the humidity and the saturation of air. In the presented sounding of Figure S1, the two lines are really close indicating a highly humid and saturated atmosphere in the given station.

For our analysis, we used the sounding from a station is located in the Darwin Airport. The station is located at -12.42°, 130.89°. The northern group of cells in the examined thunderstorm at 17 UTC was located above the sounding station.

5. MMIA instrument event definition

If there is a sudden increase in the optical signal of minimum 2 MMIA sensors, this will lead to a trigger. Sensor data are then stored for the start time, one camera frame before

the trigger to one camera frame after the last trigger in a sequence, up to a maximum of 8 camera frames. This is defined as a MMIA instrument trigger or MMIA event. The sequence contains a multitude of optical pulses from lightning.

6. Data uncertainties and induced errors

In Figure 1 of the main manuscript, for displaying purposes, blue corona discharges are projected to 17 km altitude instead of the 16 km projection altitude in the ASIM cameras. This does not affect the physical meaning of the presented cases and is only preferred in order for the events to be clearly visible in the 3D plot.

ASIM geolocation errors on ground are up to 10-20 km. This might slightly affect the position of the blue events, as indicated on the cloud top altitudes (Figure 1) and on the radar data (Figure 4). The induced uncertainties in the position are not significant for the physical meaning of the data. Furthermore, one can note that the values of Cloud Top Temperature (CTT) and Cloud Top Height (CTH) refer to a spatial resolution of 2 km, which is the resolution of the Himawari satellite.

In Figures 4b and 4c, the step feature (light blue peaks) is a result of the gridding technique of the radar data. When there is a gap between those areas, there are no observations from the discrete elevations the radar uses to sample the atmosphere and it is not certain if there is a cloud as high as either sides of those gaps.

The time delay between the initial breakdown and the optical signal is of the order of microseconds as we look at discharges at the cloud top. This is well below the absolute time accuracy of the ASIM data and can therefore be neglected as a source of timing error.

Finally, regarding the polarity and current of GLD, the reader should note that we have given the current and polarity in Table S1 and in the main manuscript as reported by the GLD network. Whether the polarity of GLD corresponds to the true polarity of the discharge is still an open question.

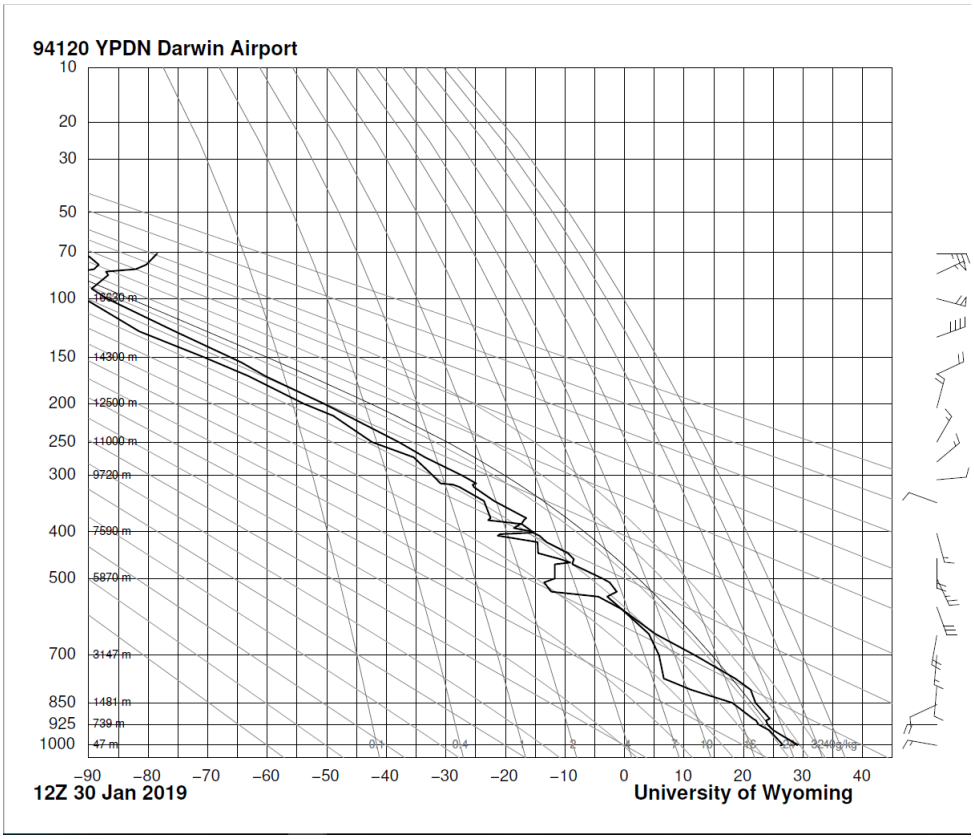

Figure S1. Atmospheric Sounding (SkewT-logP) from Darwin Aiport at 12 UTC on January 30^{th}, 2019.

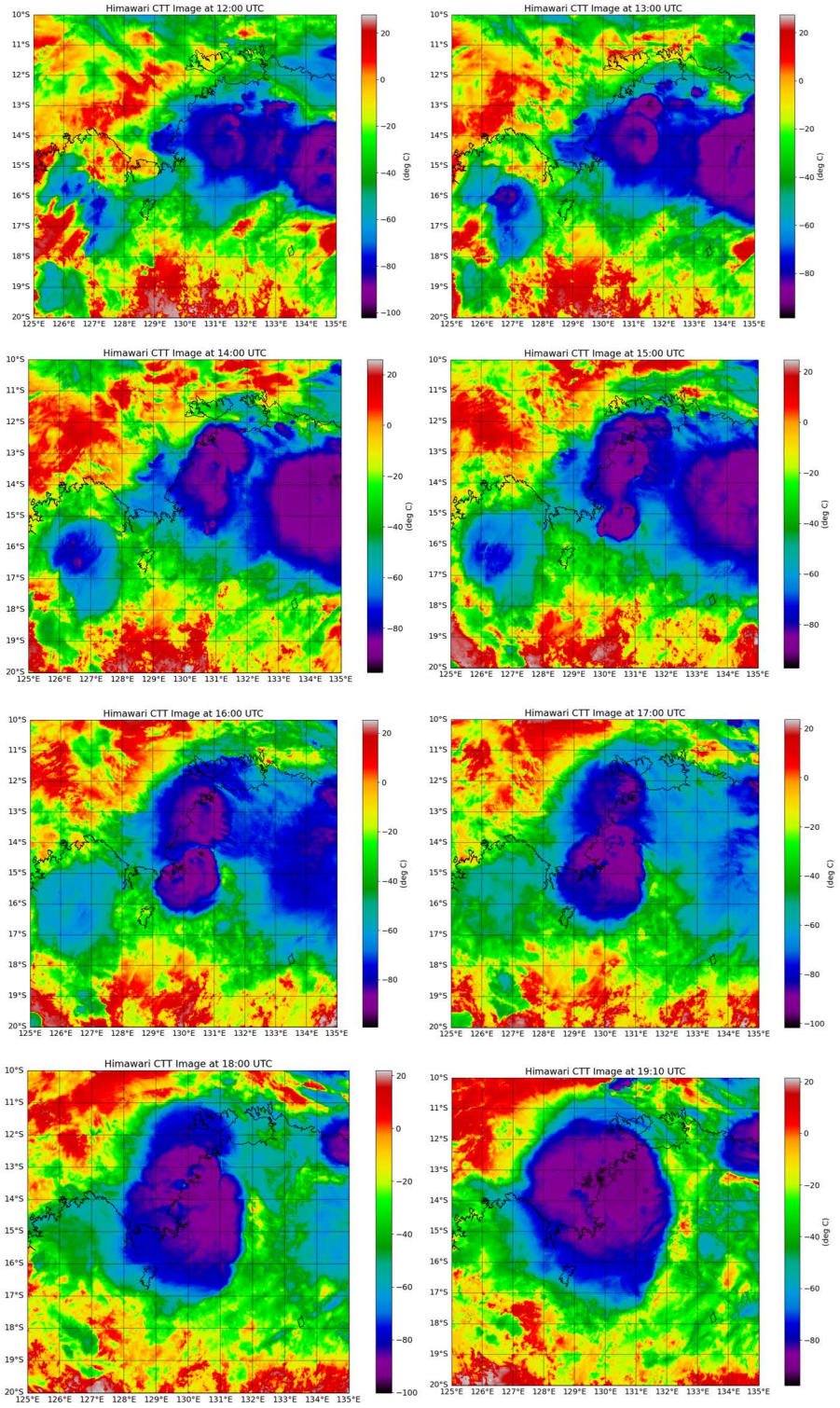

Figure S2. Storm evolution every 1 hour, from 12 UTC to 19 UTC detected by the 10.4 IR channel (Brightness Temperature) of the Himawari geostationary satellite.

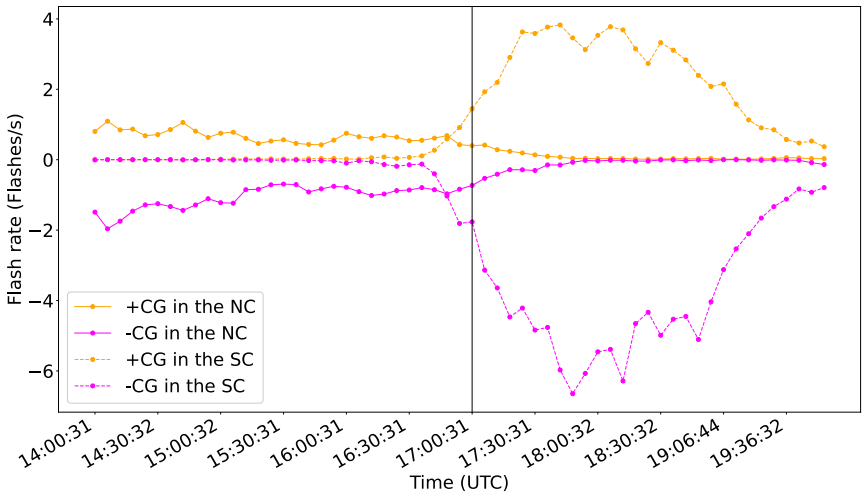

Figure S3. Flash rates of positive (orange) and negative (magenta) CGs in northern (straight line) and southern (dashed line) cells. The negative y-axis refers to the flash rates of all the negative strokes. Each point represents a radar scanning cycle (6 min) and the calculated flash rate is the average flash rate per cycle.

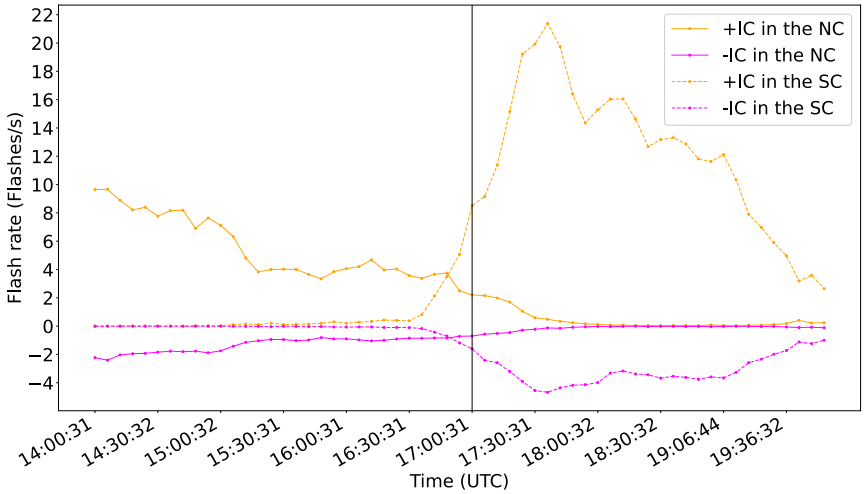

Figure S4. Flash rates of positive (orange) and negative (magenta) ICs in northern (straight line) and southern (dashed line) cells. The negative y-axis refers to the flash rates of all the negative strokes. Each point represents a radar scanning cycle (6 min) and the calculated flash rate is the average flash rate per cycle.

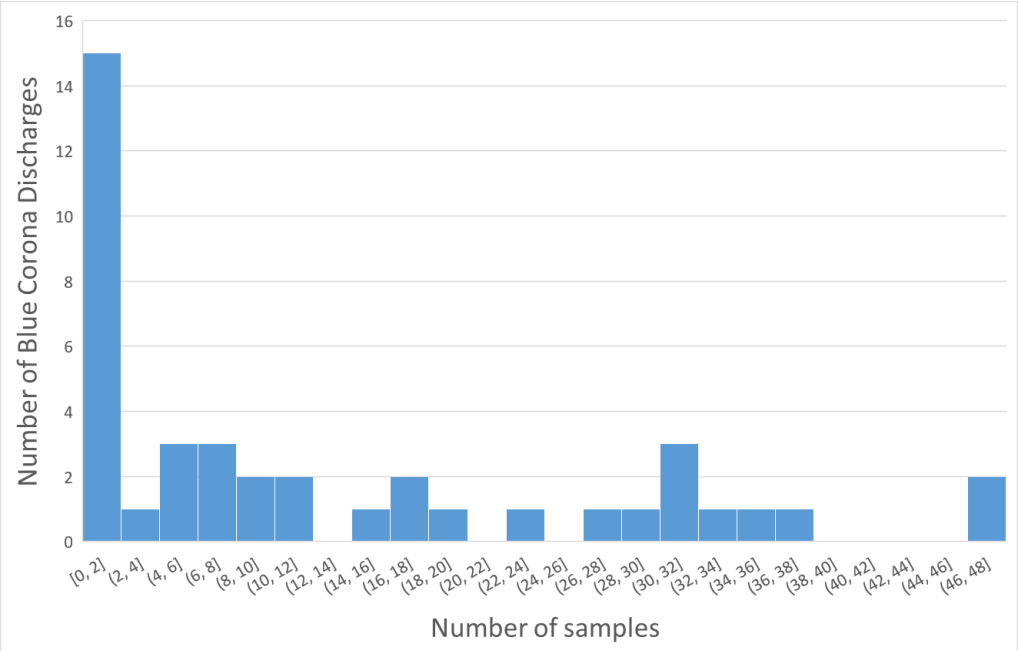

Figure S5. Rise time distribution of Blue Corona Discharge emissions for the whole storm. The horizontal axis indicates the rise time of the blue pulses expressed as a number of samples.

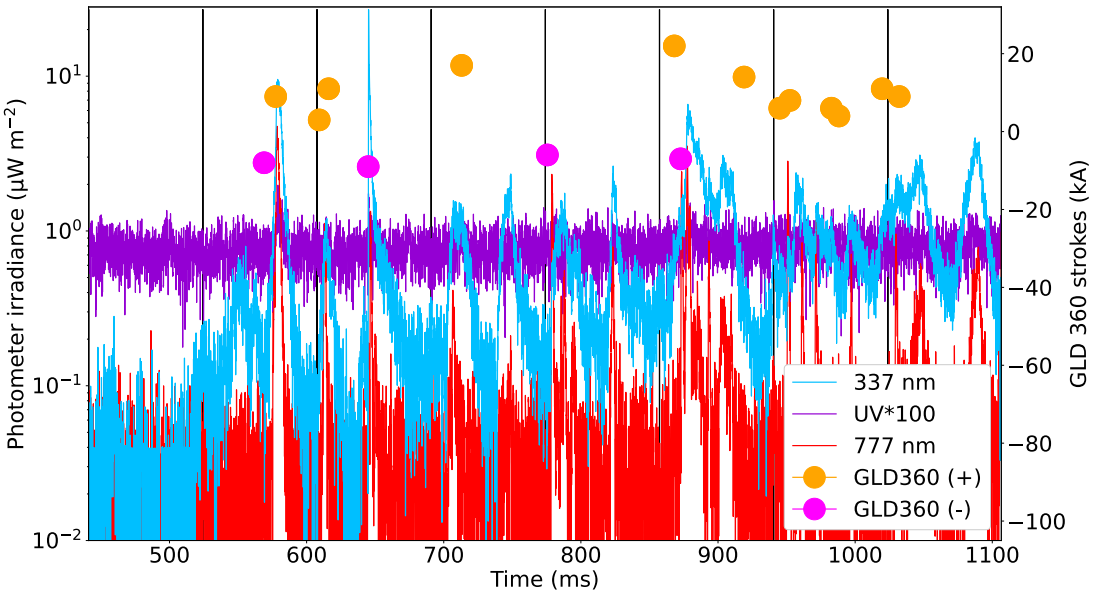

Figure S6. Blue Corona Discharge in a dissipating cell: Photometer signals of the whole MMIA event and GLD360 detections. Vertical lines mark the camera image exposure periods (∼83.3 ms). The frame of interest is Frame 3.

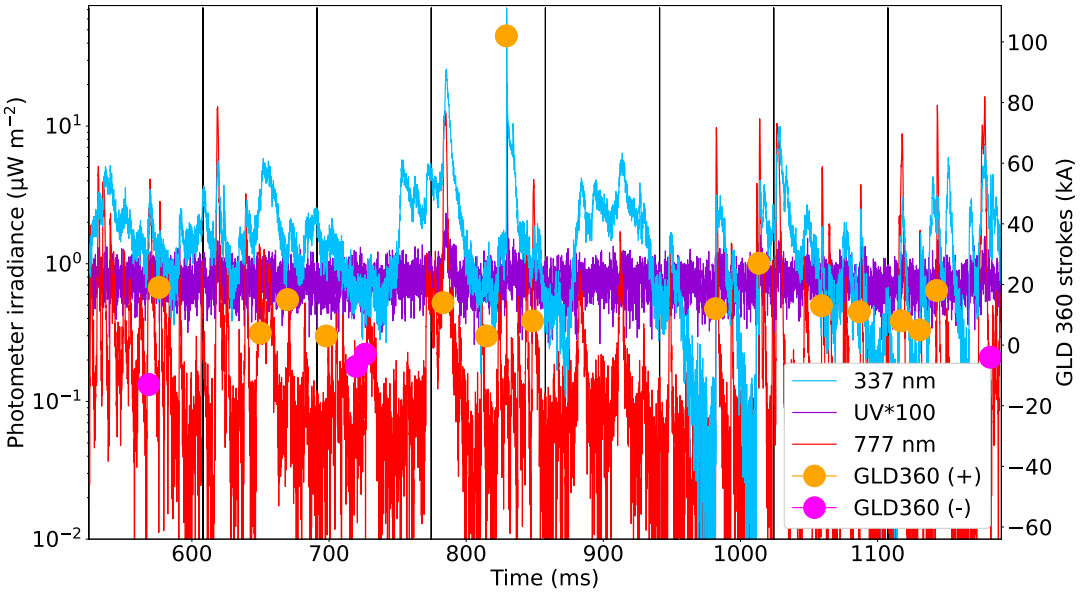

Figure S7. Blue Corona Discharges in a developing cell: Photometer signals of the whole MMIA event and GLD360 detections. Vertical lines mark the camera image exposure periods(∼83.3 ms). The frame of interest is Frame 4.

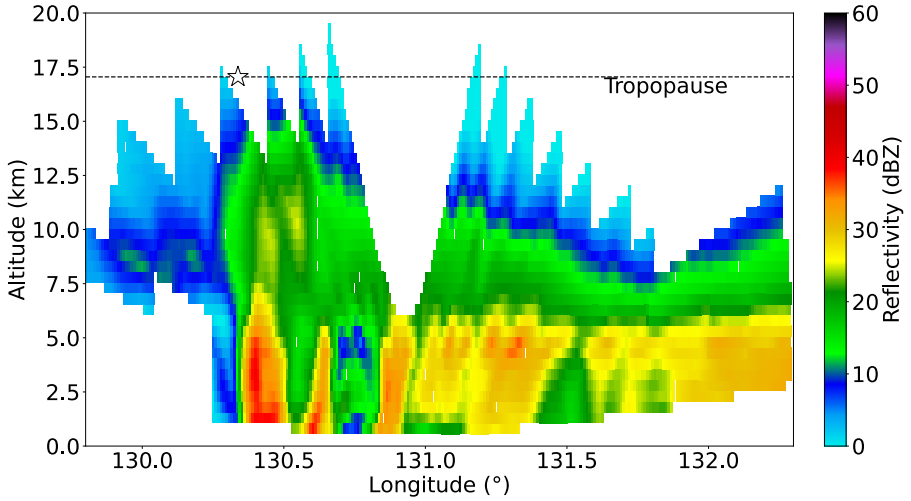

a)

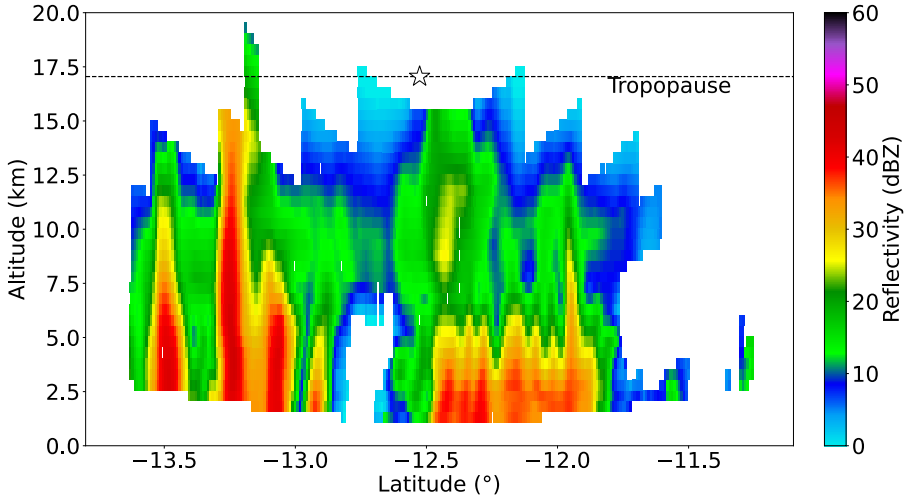

b)

Figure S8. Additional cross sections of the Blue Corona Discharges of dissipating clouds: a) The vertical cross section along -12.53° latitude (blue corona discharge latitude indicated by a white star). b) The vertical cross section along 130.34° longitude (blue corona discharge longitude indicated by a white star)

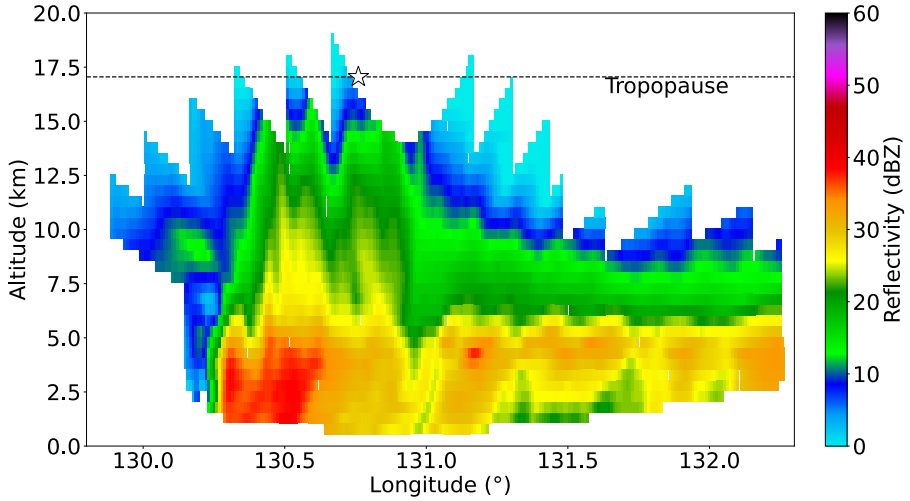

a)

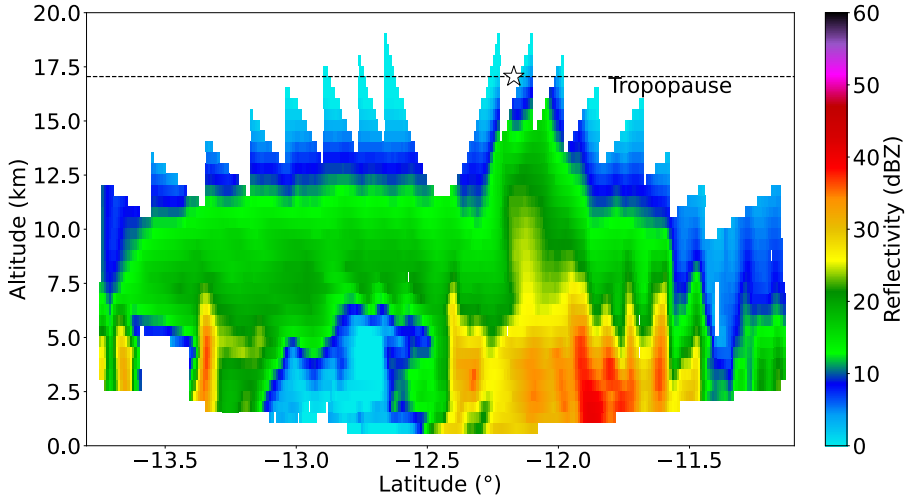

b)

Figure S9. Additional cross sections in the Blue Corona Discharges of dissipating clouds a) The vertical cross section along -12.17° latitude (blue corona discharge latitude indicated by a white star). b) The vertical cross section along 130.76° longitude (blue corona discharge longitude indicated by a white star)

Table S1. Blue corona discharge electrical and meteorological properties.

Case	Blue flash time[a] (UTC)	Blue flash rise time (μs)	Accomp. UV pulse	UV rise time (assoc. to blue) (μs)	UV rise time (assoc. to elve) (μs)	GLD or EN current (kA)	Group of cells	CTT (°C)	CTH ($\pm$ 0.5) (km)	Reflectivity (dBZ km)
1	17:02:22.645	20	-	-	-	-9	NC	-87	16.6	40
2	17:02:32.397[b]	10	single	10-20	-	-50	SC	-81	15.9	36
3	17:02:34.731	20	-	-	-	-9	NC	-84	16.3	25
4	17:02:47.708[b]	20	double	20-30	120	-54	SC	-90	17+	43
5	17:02:48.829[b]	10	double	10-20	160	102	SC	-88	16.7	38
6	17:02:50.855[b]	20	single	20-30	-	-32	NC	-89	17	38
7	17:02:54.327	10	-	-	-	-12	SC	-90	17+	-
8	17:02:59.141[b]	20	single	-	120	-144[c]	SC	-91	17+	46
9	17:03:01.899[b]	20	double	10-20	100	64	SC	-86	16.5	30
10	17:03:04.016	10	-	-	-	-19	SC	-85	16.4	49
11	17:03:20.002[b]	20	double	20-30	110	-75	SC	-88	16.8	34
12	17:03:21.392[b]	20	double	20-30	70-80	-79	SC	-86	16.5	50
13	17:03:26.741[b]	20	single	20-30	-	-54	SC	-84	16.3	28
14	17:03:34.235[b]	20	single	-	30-40	-72	SC	-89	16.9	42

Abbreviations: NC=Northern group of cells, SC=Southern group of cells,
CTT= Cloud Top Temperature, CTH=Cloud Top Height
[a]The time refers to the filtered photometer pulses.
[b]Blue flashes accompanied by UV signals.
[c]Only observation with current reported by Earth Networks.